Effects of Plasma Resonance on Surface Waves in Axially Non-Uniform Plasmas

Hitoshi HOJO, Yasuyoshi YASAKA[1)] and Atsushi MASE[2,*)]

Plasma Research Center, University of Tsukuba, Tsukuba 305-8577, Japan

[1)]*Faculty of Engineering, Kobe University, Kobe 657-8501, Japan*

[2)]*Art, Science and Technology Center for Cooperative Research, Kyushu University, Kasuga 816-8580, Japan*

(Received 17 May 2009 / Accepted 23 June 2009)

Surface waves were studied in cold cylindrical plasmas with axially non-uniform density profiles, and the eigenfrequencies and eigenfunctions for the transverse-magnetic modes of pure and hybrid surface waves were obtained numerically for collisional plasmas. The analysis of the wave equation takes into account the singularity caused by plasma resonance at which the wave frequency is equal to the local electron plasma frequency. It is shown that the axial eigenfunction of the pure surface mode peaks at the position of the plasma resonance layer, whereas the axial eigenfunction of the hybrid surface mode has two peaks at the plasma resonance layer and at the interface of the plasma and a quartz plate. Transverse-electric surface modes in axially non-uniform plasmas without plasma resonance are also analyzed.

Keywords: surface wave, plasma resonance, non-uniform plasma, transverse magnetic mode, transverse electric mode

DOI: 10.1585/pfr.5.006

1. Introduction

Surface waves have attracted much interest in the context of production and heating for processing plasmas. Earlier studies on surface waves in processing plasmas by Ghanashev *et al.* [1–4] assumed spatially uniform plasmas. However, realistic processing plasmas should be non-uniform, at least in the vicinity of a quartz plate, which is a window for incident microwave transmission due to the existence of a plasma sheath. The non-uniformity of plasma density near a quartz plate window has been observed in several experiments [5–7].

In this paper, we study surface waves in cold cylindrical plasmas having a *non-uniform* density profile. In particular, we investigate the problem of plasma resonance [8–10]. The wave equation describing transverse magnetic (TM) surface waves becomes singular on the plasma resonance surface where the wave frequency ω is equal to the local electron plasma frequency ω_{pe} when there are no collisions. This singularity leads to wave-phase mixing and then causes damping of TM surface waves. This phenomenon is the same as the resonant absorption problem of p-polarized (that is, TM) electromagnetic waves with oblique incidence in inhomogeneous plasmas. Here, we introduce a collision frequency term to avoid the singularity due to plasma resonance, for simplicity. The processing plasma is a low temperature plasma, and hence it is considered that collisions with neutral particles are not negligibly small. On the other hand, we know well that there is no plasma resonance for transverse electric (TE) electromagnetic waves.

In the following section, we show the present model for studying TM surface wave eigenmodes in a cylindrical plasma with a *non-uniform* density profile. Assuming that the plasma density is axially non- uniform (but radially uniform), we derive coupled eigenmode equations for the electric field components of TM surface waves. Section 3 attempts to solve the eigenmode equations for a plasma with an axially non-uniform density profile and discusses eigenvalues and eigenfunctions of TM surface waves of *pure* and *hybrid* types [4]. The pure surface wave is defined as an eigenmode that is evanescent in both the plasma and quartz plate regions, whereas the hybrid surface wave is a propagating mode in the quartz plate region, when the plasma is uniform. Section 4 briefly discusses TE surface waves in uniform and non-uniform plasmas. In this case, we see that no plasma resonance arises, because wave equation for TE surface waves has no singularity. Finally, the results obtained in this study are summarized in Sec. 5.

2. Equations Describing TM Surface Waves

This section describes the present plasma model for studying TM surface waves. We here assume a cold unmagnetized plasma contained by a cylindrical metallic chamber having radius a. The axial configuration of the model is shown in Fig. 1, where the metallic plate corresponding to the slot antenna is located at $z = -h$, a quartz plate of $\varepsilon_1 = 4.0$ for wave transmission exists for

*) *corresponding author's e-mail: mase@astec.kyushu-u.ac.jp*

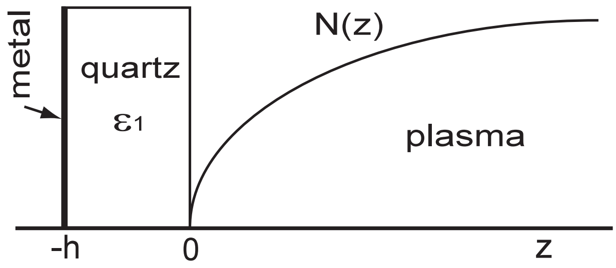

Fig. 1 Model with a non-uniform density profile.

$-h < z < 0$, and the plasma density $N(z)$ with an axially non-uniform profile exists for $z > 0$. We consider the TM surface waves being localized in the vicinity of the interface of plasma and quartz plate (i.e., $z = 0$).

Our starting point is Maxwell's equations for electromagnetic wave fields $\boldsymbol{E}$ and $\boldsymbol{B}$ and the induced current density $\boldsymbol{J}$,

$$\frac{\partial}{\partial t}\boldsymbol{B} = -\nabla\times\boldsymbol{E}, \tag{1}$$

$$\frac{\partial}{\partial t}\boldsymbol{E} = c^2\nabla\times\boldsymbol{B} - \frac{1}{\varepsilon_0}\boldsymbol{J}, \tag{2}$$

$$\frac{\partial}{\partial t}\boldsymbol{J} = \varepsilon_0\omega_{\rm pe}^2\boldsymbol{E}, \tag{3}$$

where $\omega_{\rm pe} = (e^2N/m_{\rm e}\varepsilon_0)^{1/2}$ is the electron plasma frequency, e the electric charge, $m_{\rm e}$ the electron mass, c the speed of light, and ε_0 the permittivity of free space. The above equations describe electromagnetic waves propagating in a plasma. To describe electromagnetic waves in the region of the quartz window, we use

$$\frac{\partial}{\partial t}\boldsymbol{E} = \frac{c^2}{\varepsilon_1}\nabla\times\boldsymbol{B}, \tag{4}$$

in place of Eqs. (2) and (3). If we assume an $\exp(-{\rm i}\omega t)$ dependence for $\boldsymbol{E}$ and $\boldsymbol{B}$, we obtain,

$$\nabla(\nabla\cdot\boldsymbol{E}) - \nabla^2\boldsymbol{E} - k_0^2\varepsilon_{\rm r}\boldsymbol{E} = 0, \tag{5}$$

where $\varepsilon_{\rm r}$ is given by

$$\varepsilon_{\rm r} = \begin{cases}\varepsilon_1, & -h < z < 0\\ \varepsilon_{\rm p}, & 0 < z\end{cases} \tag{6}$$

$$\varepsilon_{\rm p} = 1 - \left(\frac{\omega_{\rm pe}}{\omega}\right)^2 \tag{7}$$

and $k_0 = \omega/c$. From the x and y components of Eq. (5), we obtain

$$\frac{\partial}{\partial x}\frac{\partial E_z}{\partial z} + \frac{\partial}{\partial y}({\rm i}\omega B_z) - \left(\frac{\partial^2}{\partial z^2} + k_0^2\varepsilon_{\rm r}\right)E_x = 0, \tag{8}$$

$$\frac{\partial}{\partial y}\frac{\partial E_z}{\partial z} - \frac{\partial}{\partial x}({\rm i}\omega B_z) - \left(\frac{\partial^2}{\partial z^2} + k_0^2\varepsilon_{\rm r}\right)E_y = 0. \tag{9}$$

If we assume that the plasma density N is radially uniform and is a function of z only, then $\varepsilon_{\rm p}$ becomes a function of z only. In this case, as $\varepsilon_{\rm r}$ is a function of z only, Eqs. (8) and (9) are unified:

$$\nabla_\perp^2\frac{\partial}{\partial z}E_z - \left(\frac{\partial^2}{\partial z^2} + k_0^2\varepsilon_{\rm r}\right)\nabla_\perp\cdot\boldsymbol{E}_\perp = 0. \tag{10}$$

Also, we obtain, from the z component of Eq. (5),

$$\frac{\partial}{\partial z}\nabla_\perp\cdot\boldsymbol{E}_\perp - \left(\nabla_\perp^2 + k_0^2\varepsilon_{\rm r}\right)E_z = 0. \tag{11}$$

As the plasma is non-uniform along the z axis, we see that E_z denotes the electrostatic contribution in surface wave fields, and $\boldsymbol{E}_\perp$ expresses the electromagnetic component. If we assume $E_y = 0$, $\partial/\partial y = 0$ and $\partial/\partial x = {\rm i}k_x$, in this case, we obtain, from Eqs. (10) and (11),

$$\frac{{\rm d}^2}{{\rm d}z^2}E_z - \left(k_x^2 - k_0^2\varepsilon_{\rm p}\right)E_z + \frac{\rm d}{{\rm d}z}\left(E_z\frac{{\rm dln}\varepsilon_{\rm p}}{{\rm d}z}\right) = 0. \tag{12}$$

The solution of Eq. (12) describes TM electromagnetic waves with oblique incidence [8] and shows significant amplification of the electric wave field E_z at the plasma resonance layer of $\omega = \omega_{\rm pe}$ [9].

We here assume a separable wave form for E_z and $\nabla_\perp\cdot\boldsymbol{E}_\perp$,

$$E_z(r,\theta,z) = \psi(r,\theta)F(z), \tag{13}$$

$$\nabla_\perp\cdot\boldsymbol{E}_\perp(r,\theta,z) = \psi(r,\theta)G(z). \tag{14}$$

If we assume that ψ satisfies

$$\left(\nabla_\perp^2 + \lambda^2\right)\psi(r,\theta) = 0, \tag{15}$$

where λ is the perpendicular wavenumber obtained from the radial boundary condition:

$$E_z(r = a,\theta,z) = \psi(r = a,\theta) = 0, \tag{16}$$

we obtain the following coupled equations for $F(z)$ and $G(z)$:

$$\lambda^2\frac{\rm d}{{\rm d}z}F + \left[\frac{{\rm d}^2}{{\rm d}z^2} + k_0^2\varepsilon_{\rm r}(z)\right]G = 0, \tag{17}$$

$$\frac{\rm d}{{\rm d}z}G + \left[\lambda^2 - k_0^2\varepsilon_{\rm r}(z)\right]F = 0. \tag{18}$$

The solution of Eq. (15) is given by

$$\psi(r,\theta) = J_m(\lambda r)\left[c_1\cos(m\theta) + c_2\sin(m\theta)\right], \tag{19}$$

where J_m is the Bessel function of the first kind, c_1 and c_2 are the integration constants, and m is an integer. From the boundary condition that $E_\theta = E_z = 0$ at the metal wall $r = a$, that is, $J_m(\lambda a) = 0$, we obtain

$$\lambda = j_{mn}/a, \tag{20}$$

where j_{mn} is the n-th root of $J_m(x) = 0$. Figure 2 shows the profiles of the radial function $\psi(r,\theta)$ for $(m,n) = (1,4)$ (a) and $(m,n) = (8,1)$ (b). Hereafter, Eqs. (17) and (18) are the present basic equations for studying the axial profiles of TM surface waves.

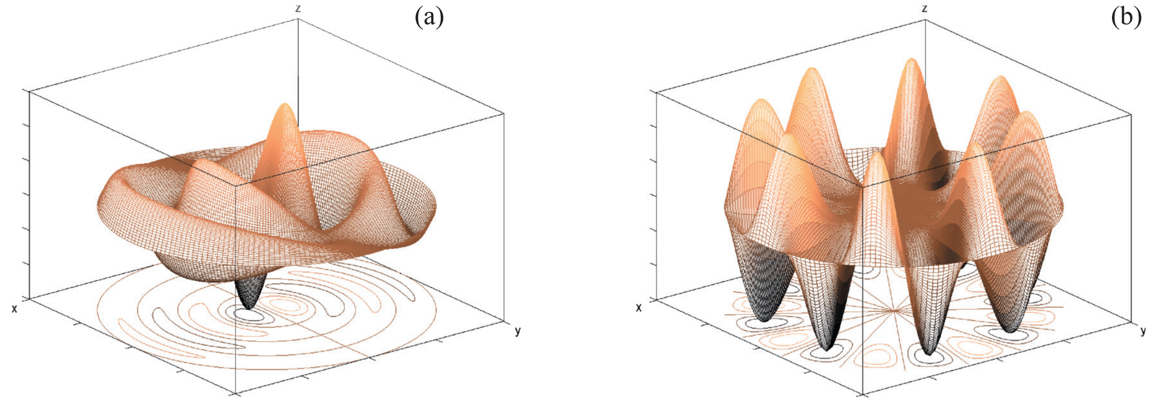

Fig. 2 Radial profiles of $\psi(r,\theta)$ with $(m,n) = (1,4)$ (a) and $(m,n) = (8,1)$ (b).

3. TM Surface Waves in Non-uniform Plasmas

As TM surface waves in a uniform plasma have been studied in detail in earlier studies [1–4], in this section, we consider TM surface waves in a non-uniform plasma. We assume the axial density profile defined as

$$N(z) = \begin{cases} N_0 \dfrac{z}{d}, & 0 < z < d \\ N_0, & z > d \end{cases} \tag{21}$$

where the plasma is non-uniform for $0 < z < d$. Such a density inhomogeneity can be generated in front of the quartz plate as a plasma sheath. We now derive a wave equation that is valid in the non-uniform plasma region $0 < z < d$. Differentiating Eq. (18) with z, we obtain

$$\frac{\mathrm{d}^2}{\mathrm{d}z^2}G + \left(\lambda^2 - k_0^2\varepsilon_\mathrm{p}\right)\frac{\mathrm{d}F}{\mathrm{d}z} - k_0^2\frac{\mathrm{d}\varepsilon_\mathrm{p}}{\mathrm{d}z}F = 0, \tag{22}$$

and substituting Eq. (17) for $\mathrm{d}F/\mathrm{d}z$ and Eq. (18) for F in Eq. (22), we can obtain a wave equation for G:

$$\frac{\mathrm{d}^2G}{\mathrm{d}z^2} + \frac{\lambda^2}{\lambda^2 - k_0^2\varepsilon_\mathrm{p}}\frac{1}{\varepsilon_\mathrm{p}}\frac{\mathrm{d}\varepsilon_\mathrm{p}}{\mathrm{d}z}\frac{\mathrm{d}G}{\mathrm{d}z} - \left(\lambda^2 - k_0^2\varepsilon_\mathrm{p}\right)G = 0. \tag{23}$$

We also obtain a wave equation for F as follows: From Eqs. (17) and (22), eliminating $\mathrm{d}^2G/\mathrm{d}z^2$, we obtain

$$G + \frac{\mathrm{d}F}{\mathrm{d}z} + \frac{1}{\varepsilon_\mathrm{p}}\frac{\mathrm{d}\varepsilon_\mathrm{p}}{\mathrm{d}z}F = 0, \tag{24}$$

and, differentiating Eq. (24) with z and using Eq. (18), we can obtain a wave equation for F:

$$\frac{\mathrm{d}^2F}{\mathrm{d}z^2} - \left(\lambda^2 - k_0^2\varepsilon_\mathrm{p}\right)F + \frac{\mathrm{d}}{\mathrm{d}z}\left(F\frac{\mathrm{d}\ln\varepsilon_\mathrm{p}}{\mathrm{d}z}\right) = 0. \tag{25}$$

This wave equation is essentially the same as Eq. (12) in the previous section.

We next try to solve the wave equation for G in the non-uniform plasma region, where the axial boundary conditions for G are $G(z=-h) = 0$ and $G(z=+\infty) = 0$. We assume $\lambda^2 \gg |k_0^2\varepsilon_\mathrm{p}|$, which is justified for both low-density plasmas and high m (or n) modes. Using this approximation, from $\lambda^2/(\lambda^2 - k_0^2\varepsilon_\mathrm{p}) \approx 1$, Eq. (23) is reduced to

$$\frac{\mathrm{d}^2G}{\mathrm{d}z^2} + \frac{1}{\varepsilon_\mathrm{p}}\frac{\mathrm{d}\varepsilon_\mathrm{p}}{\mathrm{d}z}\frac{\mathrm{d}G}{\mathrm{d}z} - \lambda^2G = 0, \tag{26}$$

and, from Eq. (18), F is approximated by

$$F = -\frac{1}{\lambda^2}\frac{\mathrm{d}}{\mathrm{d}z}G. \tag{27}$$

We see that Eq. (26) becomes singular at $z_\mathrm{r} = d(\omega/\omega_{\mathrm{p}0})^2$, as $\varepsilon_\mathrm{p}(z) = 1 - (\omega_{\mathrm{p}0}/\omega)^2(z/d)$, where $\omega_{\mathrm{p}0} = (e^2N_0/m_\mathrm{e}\varepsilon_0)^{1/2}$. This singularity of $\varepsilon_\mathrm{p} = 0$ in Eq. (26) corresponds to plasma resonance. We mention here that Eq. (26) is quite similar to the wave equation describing the spatial resonance of Alfvén waves discussed by L. Chen and A. Hasegawa [11]. Thus, the plasma resonance due to the singularity of $\varepsilon_\mathrm{p} = 0$ causes the phase mixing of waves, resulting in wave damping. However, for simplicity, we introduce the collision frequency term to avoid the singularity of the plasma resonance. We then replace $\varepsilon_\mathrm{p}(z)$ of Eq. (7) by

$$\varepsilon_\mathrm{p}(z) = 1 - \frac{\omega_{\mathrm{p}0}^2}{\omega(\omega + \mathrm{i}\nu)}\frac{N(z)}{N_0}, \tag{28}$$

where ν is the collision frequency. The solution of Eq. (26) is given by the modified Bessel function of the first and second kinds, i.e., I_0 and K_0. Then we have, for a pure TM surface wave,

$$F(z) = \begin{cases} \alpha_1\cosh\left[p_1(z+h)\right], & -h < z < 0 \\ -\dfrac{1}{\lambda}\left[\alpha_2I_1(\xi) - \alpha_3K_1(\xi)\right], & 0 < z < d \\ \alpha_4\exp\left(-p_2z\right), & z > d \end{cases} \tag{29}$$

$$G(z) = \begin{cases} -\alpha_1p_1\sinh\left[p_1(z+h)\right], & ad - h < z < 0 \\ \alpha_2I_0(\xi) + \alpha_3K_0(\xi), & 0 < z < d \\ \alpha_4p_2\exp\left(-p_2z\right), & z > d \end{cases} \tag{30}$$

with

$$\xi = \lambda\left[z - d\omega(\omega + \mathrm{i}\nu)/\omega_{\mathrm{p}0}^2\right], \tag{31}$$

where α_1, α_2, α_3, and α_4 are integration constants, and p_1 and p_2 are defined in the previous section. Thus, three of α_1, α_2, α_3, and α_4 and the dispersion equation for pure TM surface wave can be obtained from the continuity conditions at $z = 0$ and $z = d$, i.e.,

$$\varepsilon_1 F(+0) = \varepsilon_p F(-0) \text{ and } G(-0) = G(+0),$$
$$F(d+0) = F(d-0) \text{ and } G(d-0) = G(d+0). \quad (32)$$

From the above continuity conditions, we can obtain the dispersion equations of pure TM surface modes as

$$\frac{t_2 I_1(\xi_2) - I_0(\xi_2)}{t_2 K_1(\xi_2) + K_0(\xi_2)} = \frac{t_1 I_1(\xi_1) + I_0(\xi_1)}{t_1 K_1(\xi_1) - K_0(\xi_1)}, \quad (33)$$

with

$$t_1 = \frac{p_1}{\lambda\varepsilon_1}\tanh(p_1 h),\ t_2 = -\frac{p_2}{\lambda}. \quad (34)$$

$$\xi_1 = \lambda d\frac{\omega(\omega + \mathrm{i}\nu)}{\omega_{\mathrm{p0}}^2},\ \xi_2 = \lambda d\left[1 - \frac{\omega(\omega + \mathrm{i}\nu)}{\omega_{\mathrm{p0}}^2}\right]. \quad (35)$$

On the other hand, for hybrid TM surface waves, the solutions of F and G for $0 < z < d$ are replaced by

$$F(z) = \alpha_1 \cos[q_1(z+h)], \quad 0 < z < d,$$
$$G(z) = \alpha_1 q_1 \sin[q_1(z+h)], \quad 0 < z < d,$$

where q_1 is given by $q_1 = \sqrt{k_0^2\varepsilon_1 - \lambda^2}$. Similarly, we obtain the dispersion equation for hybrid TM surface wave, that is, Eq. (33) with

$$t_1 = -\frac{q_1}{\lambda\varepsilon_1}\tan(q_1 h), \quad t_2 = -\frac{p_2}{\lambda}. \quad (36)$$

For the collision frequency, we assume that $\nu a/c = 0.01N_0/N^*$, N^* being the density at $(\omega_{\mathrm{p0}}a/c)^2 = 50$. Figure 3 shows the eigenfrequencies and damping rates of pure TM_{81} and TM_{16} surface modes as a function of $(\omega_{\mathrm{p0}}a/c)^2$, where the parameters are $h/a = 0.2$ and $d/a = 0.3$, with $j_{81} = 12.225$ and $j_{16} = 19.616$. We observe that the damping rate $\mathrm{Im}(\omega)$ is almost linearly proportional to $(\omega_{\mathrm{p0}}a/c)^2$. From the numerical calculation for the case of $\nu a/c = 0.1N_0/N^*$, we find that the damping rate is also linearly proportional to the collision frequency ν. Figure 4 shows the eigenfunctions G and F of the pure TM_{81} mode for $(\omega_{\mathrm{p0}}a/c)^2 = 50$, where the other parameters are the same as those in Fig. 3. We observe that the eigenfunction $|G|$ of the pure TM_{81} surface mode has a peak at the position $z_r = d(\omega/\omega_{\mathrm{p0}})^2$ of the plasma resonance satisfying $\varepsilon_p(z) = 0$ for $\nu = 0$. On the other hand, the eigenfunction G of pure TM surface mode in a uniform plasma has a peak on the interface between the quartz-plate and plasma. We observe that the eigenfunction $|F|$ peaks at the position z_r of the plasma resonance, and there is a jump in $|F|$ at the interface $z = 0$ because of Eq. (32). Comparison between F and G suggests that the eigenfunction F is more sharply localized than that of G.

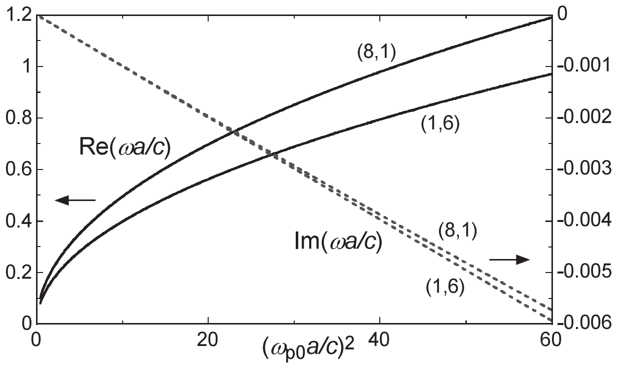

Fig. 3 Eigenfrequencies and damping rates of pure TM_{81} and TM_{16} surface modes, where $h/a = 0.2$ and $d/a = 0.3$.

In the case of hybrid TM surface waves, we have to solve the dispersion equation of Eq. (33) with Eq. (36) to obtain the eigenfrequencies. As $p_2 > 0$ and $q_1 > 0$ for hybrid TM surface waves, the wave frequency ω must satisfy

$$\lambda a/\sqrt{\varepsilon_1} < \omega a/c < \sqrt{\left(\omega_{\mathrm{p0}}a/c\right)^2 + (\lambda a)^2}$$

when ω is real. However, if we assume the existence of plasma resonance in the non-uniform plasma region, as ω must satisfy $\omega < \omega_{\mathrm{p0}}$, the wave frequency ω is in the range

$$\lambda a/\sqrt{\varepsilon_1} < \omega a/c < \omega_{\mathrm{p0}}a/c.$$

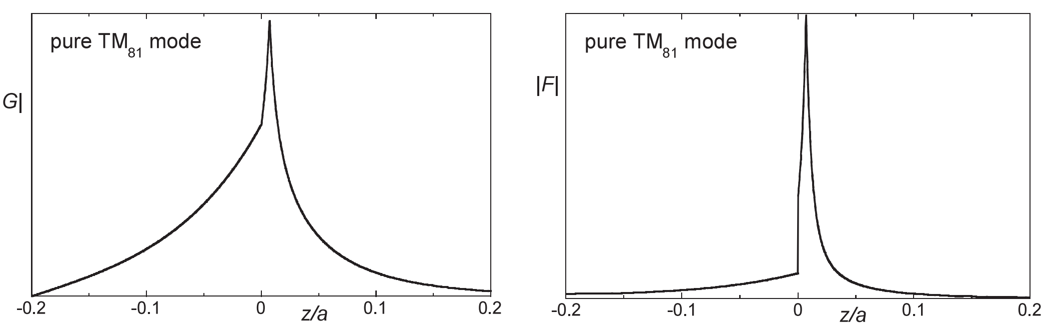

Fig. 4 Eigenfunctions $|G|$ and $|F|$ of pure TM_{81} surface mode for $(\omega_{\mathrm{p0}}a/c)^2 = 50$, where $h/a = 0.2$ and $d/a = 0.3$.

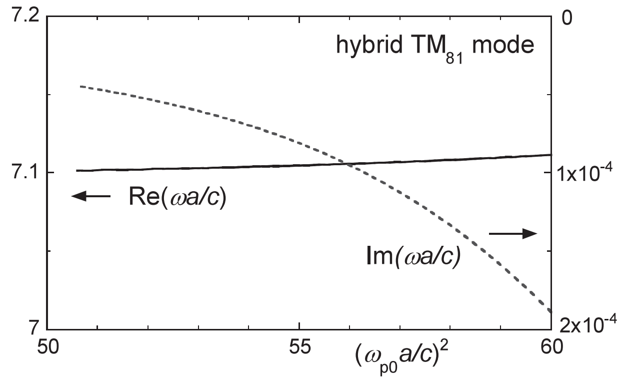

Fig. 5 Eigenfrequency of hybrid TM_{81} surface mode, where $h/a = 0.2$ and $d/a = 0.3$.

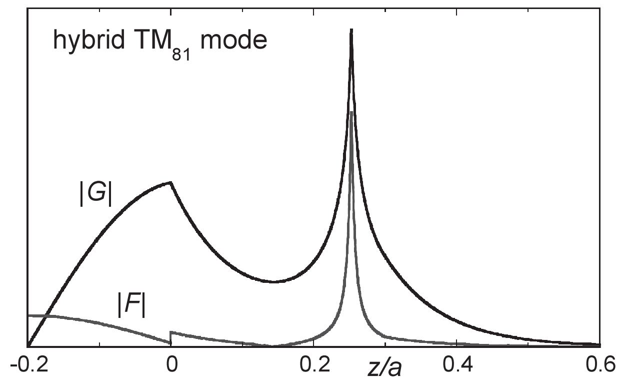

Fig. 7 Eigenfunctions $|G|$ and $|F|$ of hybrid TM_{81} surface mode for $(\omega_{\mathrm{p0}}a/c)^2 = 60$, where $h/a = 0.2$ and $d/a = 0.3$.

Figure 5 shows the lowest eigenfrequency of a hybrid TM_{81} surface wave, where the parameters are the same as those in Fig. 3. In this case, we observe that the real frequency of the hybrid surface mode depends weakly on $(\omega_{\mathrm{p0}}a/c)^2$, and the damping rate is much smaller than that of the pure surface mode. Figure 6 shows the axial eigenfunctions G and F of the lowest hybrid TM_{81} surface mode for $(\omega_{\mathrm{p0}}a/c)^2 = 55$, where the other parameters are the same as those in Fig. 5. For hybrid surface wave, two peaks appear in the axial wave profile of $|G|$. One peak is localized at the plasma resonance point of $\varepsilon_{\mathrm{p}}(z) = 0$, and the other on the interface between the plasma and quartz plate. On the other hand, the wave function G for pure surface wave has a peak only at the plasma resonance point, as shown in Fig. 4. The axial eigenfunction $|F|$ peaks at the plasma resonance point and has a discontinuity on the plasma-quartz plate interface, as shown in Fig. 5. Figure 7 shows the axial eigenfunctions $|G|$ and $|F|$ of the lowest hybrid TM_{81} surface mode at $(\omega_{\mathrm{p0}}a/c)^2 = 60$, where the other parameters are the same as those in Fig. 6. Although, in this case, we observe two peaks in $|G|$, the peak at the plasma resonance point is higher than that on the plasma-quartz plate interface (Fig. 6). Therefore, we observe that the detailed structure of the two peaks depends on the value of $(\omega_{\mathrm{p0}}a/c)^2$. We note here that Eq. (23) and Figs. 2 and 3 in Ref. [10] should be replaced by Eq. (34) and Figs. 3 and 4 of this article, respectively.

4. TE Surface Waves in Non-uniform Plasmas

In this section, we study TE surface waves in non-uniform plasmas, although in this case, there is no plasma resonance corresponding to a singularity in the wave equation. From Eqs. (1) to (3), the TE surface waves are described by

$$\left(\nabla_\perp^2 + \frac{\partial^2}{\partial z^2} + k_0^2\varepsilon_{\mathrm{r}}\right) B_z = 0. \tag{37}$$

Using a method similar to that used for TM surface waves and assuming the following separable form,

$$B_z(r,\theta,z) = \psi(r,\theta)R(z), \tag{38}$$

we can obtain the below equation for $R(z)$:

$$\frac{\mathrm{d}^2}{\mathrm{d}z^2}R - \left[\lambda^2 - k_0^2\varepsilon_{\mathrm{r}}(z)\right]R = 0. \tag{39}$$

From Eq. (39), we see that plasma resonance does not appear for TE surface waves, although a cutoff can appear at

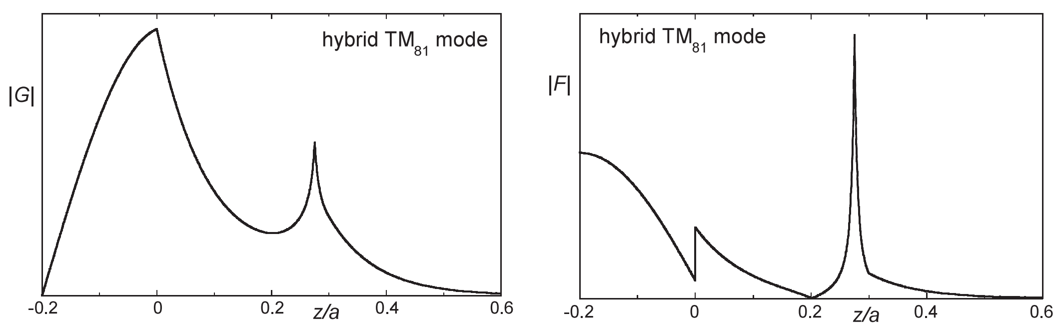

Fig. 6 Eigenfunctions $|G|$ and $|F|$ of hybrid TM_{81} surface mode for $(\omega_{\mathrm{p0}}a/c)^2 = 55$, where $h/a = 0.2$ and $d/a = 0.3$.

$\lambda^2 = k_0^2\varepsilon_r$. For TE modes, the radial boundary condition, i.e., $E_\theta = 0$ at $r = a$, is reduced to

$$\partial\psi/\partial r|_{r=a} = 0. \tag{40}$$

From Eq. (40), we obtain

$$\lambda = j'_{mn}/a, \tag{41}$$

where j'_{mn} is the n-th root of $\mathrm{d}J_m/\mathrm{d}r = 0$.

We now consider TE surface waves in an axially non-uniform plasma, assuming the same density profile discussed in the previous section. In this case, for $0 < z < d$, Eq. (39) is reduced to

$$\frac{\mathrm{d}^2}{\mathrm{d}\zeta^2}R - \zeta R = 0, \tag{42}$$

$$\zeta = \left[\left(\omega_{\mathrm{p0}}/c\right)^2/d\right]^{\frac{1}{3}}\left[z + d\left(\lambda^2 - k_0^2\right)\left(c/\omega_{\mathrm{p0}}\right)^2\right]. \tag{43}$$

The solution of Eq. (42) is given by the Airy functions $\mathrm{Ai}(\zeta)$ and $\mathrm{Bi}(\zeta)$, which are expressed in terms of the modified Bessel functions as [12]

$$\mathrm{Ai}(\zeta) = (1/\pi)\sqrt{\zeta/3}K_{1/3}\left(2\zeta^{3/2}/3\right), \tag{44}$$

$$\mathrm{Bi}(\zeta) = \sqrt{\zeta/3}\left[I_{-1/3}\left(2\zeta^{3/2}/3\right) + I_{1/3}\left(2\zeta^{3/2}/3\right)\right]. \tag{45}$$

Therefore, the solution of Eq. (39) for a pure TE surface wave is obtained by

$$R(z) = \begin{cases} \alpha_1 \sinh\left[p_1(z+h)\right], & -h < z < 0 \\ \alpha_2\mathrm{Ai}(\zeta) + \alpha_3\mathrm{Bi}(\zeta), & 0 < z < d \\ \alpha_4 \exp\left(-p_2 z\right), & z > d \end{cases} \tag{46}$$

and, for a hybrid surface wave by

$$R(z) = \begin{cases} \alpha_1 \sin\left[p_1(z+h)\right], & -h < z < 0 \\ \alpha_2\mathrm{Ai}(\zeta) + \alpha_3\mathrm{Bi}(\zeta), & 0 < z < d \\ \alpha_4 \exp\left(-p_2 z\right), & z > d \end{cases} \tag{47}$$

where three of α_1, α_2, α_3, and α_4 and the dispersion equation for TE surface waves are obtained from the continuity conditions at $z = 0$ and $z = d$, i.e.,

$$R(+0) = R(-0), \text{ and } R'(+0) = R'(-0), \tag{48}$$

and

$$R(d+0) = R(d-0), \text{ and } R'(d+0) = R'(d-0). \tag{49}$$

We then have

$$\frac{t_2\mathrm{Ai}(z=d) - \mathrm{Ai}'(z=d)}{t_1\mathrm{Ai}(z=0) - \mathrm{Ai}'(z=0)} = \frac{t_2\mathrm{Bi}(z=d) - \mathrm{Bi}'(z=d)}{t_1\mathrm{Bi}(z=0) - \mathrm{Bi}'(z=0)}, \tag{50}$$

with, for pure TE surface waves,

$$t_1 = \frac{p_1}{s}\coth(p_1 h), \quad t_2 = -\frac{p_2}{s}, \tag{51}$$

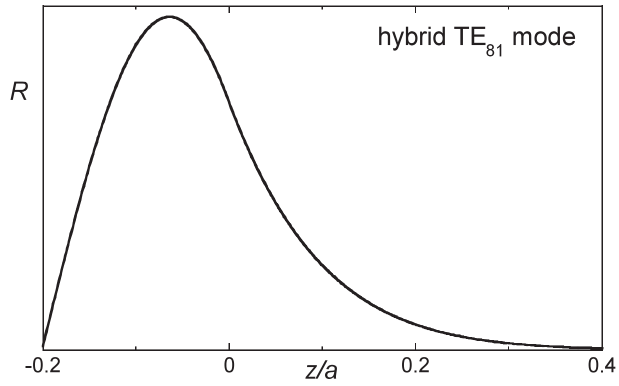

Fig. 8 Axial eigenfunction R of hybrid TE_{81} surface mode, where $h/a = 0.2$, $d/a = 0.3$ and $\omega_{\mathrm{p0}}a/c = 10$. In this case, the eigenfrequency is $\omega a/c = 8.30$.

and for hybrid TE surface waves,

$$t_1 = \frac{q_1}{s}\cot(q_1 h), \quad t_2 = -\frac{p_2}{s}, \tag{52}$$

where $s = \left[\left(\omega_{\mathrm{p0}}/c\right)^2/d\right]^{1/3}$.

For pure TE surface waves, we observe that the numerical computation of Eq. (50), using Eq. (51), yields no solution. This is indicated in Ref. [1] for the case of uniform plasmas. On the other hand, we clearly observe that hybrid-mode solutions of the TE surface wave in Eq. (50) with Eq. (52) exist. Figure 8 shows the axial eigenfunction R of the lowest hybrid TE_{81} surface mode, where $h/a = 0.2$, $d/a = 0.3$, and $\omega_{\mathrm{p0}}a/c = 10$ are assumed. In this case, the eigenfrequency is $\omega a/c = 8.30$ for $\omega_{\mathrm{p0}}a/c = 10$, where we assumed $\nu = 0$, as there is no singularity for TE surface waves. We see that the eigenfunction R decays exponentially in the plasma region.

5. Summary

We have studied TM and TE surface waves in plasmas with axially non-uniform density profiles. For TM surface waves, we derived the eigenmode equation describing the axial wave profile. The eigenmode equation becomes singular at the plasma resonance point, where the wave frequency is equal to the local electron plasma frequency, when the plasma is collision-free. By solving the eigenmode equation for collisional plasmas, we obtained the eigenfrequencies and axial eigenfunctions of pure and hybrid TM surface waves. We found that the axial eigenfunction of the pure TM surface mode peaks strongly at the plasma resonance point; on the other hand, the peak in the eigenfunction of the hybrid TM surface mode occurred both at the plasma resonance point and at the interface between the plasma and quartz plate. We also obtained the axial eigenfunction of the hybrid TE surface wave in axially non-uniform plasmas without plasma resonance.

Acknowledgment

This work was partly supported by a Grant-in-Aid for Scientific Research from the Ministry of Education, Culture, Sports and Technology of Japan.

[1] I. Ghanashev, M. Nagatsu and H. Sugai, Jpn. J. Appl. Phys. **36**, 337 (1997).

[2] I. Ghanashev, M. Nagatsu, S. Morita and H. Sugai, J. Vac. Sci. Techno. A **16**, 1537 (1998).

[3] E. Abdel-Fattah, I. Ghanashev and H. Sugai, Jpn. J. Appl. Phys. **39**, 4181 (2000).

[4] T. Yamauchi, K. Aoki, M. Kanoh and H. Sugai, J. Vac. Sci. Technol. A **19**, 2433 (2001).

[5] J. Kudela, T. Terebessy and M. Kando, Appl. Phys. Lett. **76**, 1249 (2000).

[6] T. Terebessy, M. Kando and J. Kudela, Appl. Phys. Lett. **77**, 2825 (2000).

[7] T.J. Wu, W.J. Guan, C.M. Tsai, W.Y. Yeh and C.S. Kou, Phys. Plasmas **8**, 3195 (2001).

[8] V.L. Ginzburg, *The Propagation of Electromagnetic Waves in Plasmas* (Pergamon, Oxford, 1964).

[9] Y. Yasaka and H. Hojo, Phys. Plasmas **7**, 1601 (2000).

[10] H. Hojo, A. Shimamura, N. Uchida, Y. Yasaka and A. Mase, J. Plasma Fusion Res. **80**, 719 (2004).

[11] L. Chen and A. Hasegawa, Phys. Fluids **17**, 1399 (1974).

[12] M. Abramowitz *et al.*, *Handbook of Mathematical Functions with Formulas, Graphs, and Mathematical Tables* (Dover, 1999).